Original Article

Acupuncture and Herbal Medicine

OPEN

Comprehensive profiling of Lingzhihuang capsule by liquid chromatography coupled with mass spectrometry-based molecular networking and target prediction

Mengliang Huang[1], Sijia Yu[2], Qing Shao[2], Hao Liu[2], Yingchao Wang[2], Hongzhang Chen[3], Yansheng Huang[3], Yi Wang[1,2,*]

Abstract

Objective: Lingzhihuang capsule (LZHC) is a natural product that consists of 10 commonly used medicinal plants, and it is used in traditional Chinese medicine to promote people's overall health. Previously, LZHC was successfully used as adjuvant therapy for treating patients with cancer. However, the chemical constituents of LZHC and their potential biological functions remain unclear. The aim of this study is to investigate the major bioactive compounds in LZHC and predict their pharmacological targets.

Methods: The LZHC constituents were putatively identified by ultra-high performance liquid chromatography coupled with time-of-flight mass spectrometry combined with mass spectrometry-based molecular networking. The targets were predicted using SwissTargetPrediction software, and the associated gene ontology and Kyoto encyclopedia of genes and genomes pathways were analyzed using the Database for Annotation, Visualization, and Integrated Discovery. The mass spectrometry-based molecular network and compound-target-pathway network were constructed using Cytoscape 3.8.0 software.

Results: We putatively identified 94 compounds of LZHC by mass spectrometry-based molecular networking, including triterpene (the main structural type) and other clusters (ie, flavonoids and organic acids). Our results suggested that multiple pivotal targets were regulated by LZHC, including tumor necrosis factor, nitric oxide synthase 2, glucocorticoid receptor, estrogen receptor, 3-oxo-5-alpha-steroid 4-dehydrogenase 2, prostaglandin e2 receptor ep4 subtype, estrogen receptor beta, phosphatidylinositol 4,5-bisphosphate 3-kinase catalytic subunit alpha isoform, mitogen-activated protein kinase 3, and rac-alpha serine, which are related to signal transduction, positive regulation of transcription from RNA polymerase II promoters, oxidation-reduction processes, inflammatory responses, and other biological processes. Functional annotation of those targets suggested that several signaling pathways may be regulated by LZHC, such as cancer-related proteoglycans, the PI3K-Akt-signaling pathway, and the cAMP-signaling pathway.

Conclusions: Our findings reveal the chemical constituents of LZHC and provided scientific support for the efficacy of LZHC in terms of immune regulation, anti-aging, and tumor suppression.

Keywords: Lingzhihuang capsule, Molecular networking, Network pharmacology, UPLC-Q-TOF/MS

Graphical abstract: http://links.lww.com/AHM/A12

Introduction

Lingzhihuang capsule (LZHC) is a natural product used to promote human health that consists of *Ganoderma lucidum, Atractylodes macrocephala, Polygonatum sibiricum, Lycium barbarum, Coix lacryma-jobi, Poria cocos, Ophiopogon japonicus, Cuscuta chinensis, Schisandra chinensis*, and *Glycyrrhiza uralensis* Fisch. Among these medicinal herbs, previous pharmacological data have suggested that *G. lucidum*, *G. uralensis* Fisch, *C. chinensis*, and *P. cocos* exert anti-inflammatory, antitumor, and anti-aging effects[1–3]. For example, they have demonstrated primary or auxiliary effects against gastric and throat cancer[4], acute pancreatitis[5], breast cancer[6], liver disease[7], diabetes[8], dementia[9], and other diseases. Previously, LZHC was recommended for middle-aged or elderly people with a weak physique, and for patients with cancer. Data from a previous report indicated that combined use of Yanggujian and LZHC was more beneficial when managing patients with *qi*-deficiency syndrome[10]. However, the chemical composition and downstream targets of LZHC remain elusive, and little scientific evidence is available.

[1] State Key Laboratory of Component-Based Chinese Medicine, Tianjin University of Traditional Chinese Medicine, Tianjin, China; [2] Pharmaceutical Informatics Institute, College of Pharmaceutical Sciences, Zhejiang University, Hangzhou, China; [3] Infinitus (China) Company, Ltd., Guangzhou, China

[*] Corresponding author. Yi Wang, State Key Laboratory of Component-based Chinese Medicine, Tianjin University of Traditional Chinese Medicine, Tianjin 301617, China; Pharmaceutical Informatics Institute, College of Pharmaceutical Sciences, Zhejiang University, Hangzhou 310058, China, E-mail: zjuwangyi@zju.edu.cn.

Acupuncture and Herbal Medicine (2022) 2:1

Received 27 January 2021 / Accepted 3 June 2021

http://dx.doi.org/10.1097/HM9.0000000000000012

Liquid chromatography-coupled with mass spectrometry (LC-MS) has become a powerful tool for revealing the complex chemical compositions of herbal medicines. For example, Fu et al.[11] analyzed the chemical constituents of Xuefu Zhuyu decoction by ultra-performance liquid chromatography (UPLC) coupled to ion-trap time-of-flight (TOF)-MS and inferred 34 compounds. Likewise, Yang et al.[12] studied the chemical constituents of Glycyrrhizae Radix et Rhizoma in Pinelliae Rhizoma Praeparatum (PRP) by UPLC coupled to quadrupole (Q)-TOF-MS/MS, and identified 15 chemical compounds present in PRP licorice. Yang et al.[13] also used UPLC-Q-TOF/MS to study Suanzaoren decoction, from which 22 compounds were identified or inferred. Moreover, MS-based molecular networking (MN) is an emerging tool used to accelerate the pace of analyzing natural plants. Wang et al.[14] combined MS-MN with a virtual screening-affinity MS-screening technique to exa mine the active components from 12 anti-cancer Chinese medicinal herbs, and two compounds were identified that regulate the activity of the Ras protein. This method significantly improved the throughput of ligand screening and the accuracy of the screening results. Yang et al.[15] used LC-high resolution MS combined with MS-MN to study the chemical constituents and pharmacological mechanism of Qingfei Paidu decoction (a traditional Chinese medicine prescription that has been used for clinical treatment of coronavirus disease 2019) and 129 compounds were identified and classified.

Those applications suggest that integrated LC-MS analysis and MN can be used to efficiently determine the complex chemical composition of LZHC. Network pharmacology[16] is a new strategy that combines pharmacology with network analysis, which was originally proposed by Hopkins in 2007. The strategy involves searching for the potentially active ingredients of the mixture through network databases, such as the Traditional Chinese Medicine Systems Pharmacology (TCMSP) database, followed by predicting their targets and relevant diseases, as well as signal-pathway enrichment analysis to establish network relationships or drug-gene-target-disease interactions. The possible effective components of drugs and their molecular mechanisms can be predicted by the network relationship, which provides a basis for further research and applications. This method is especially suitable for studying compound prescriptions used in traditional Chinese medicine for which the pharmacological mechanism involves multiple components, targets, and pathways. Therefore, network pharmacology has become a popular approach for studying the molecular mechanisms of traditional Chinese medicines in recent years[17–20].

In this study, the chemical components and potential biological mechanisms of LZHC were comprehensively analyzed by UPLC-Q-TOF/MS combined with network pharmacology. MN was employed to process the LC-MS data and classify the identified compounds into different categories, based on MS/MS similarity. Furthermore, the potential targets of the major constituents were predicted by network pharmacology. Functional-annotation results indicated that the pivotal targets regulated by LZHC include tumor necrosis factor (TNF), nitric oxide synthase 2 (NOS2), glucocorticoid receptor (NR3C1), and rac-alpha serine (AKT1), which suggested that multiple pathways associated with cancer, aging, and inflammation may be regulated by LZHC. Our findings provided scientific support for the efficacy of LZHC in terms of immune regulation, anti-aging, and combinatory therapy against tumors.

Materials and methods

Materials and reagents

The reference compounds quercetin, hyperoside, liquiritin apioside, licochalcone A, glycyrrhizic acid, and liquiritigenin were purchased from Shanghai Yuanye Biotechnology Co., Ltd. (Shanghai, China). Chlorogenic acid, isoliquiritin apioside, 5-hydroxymethylfurfural, 3,4-dihydroxybenzaldehyde, liquiritin, isoliquiritin, kaempferol, ophiopogonin D, methylophiopogonanone A, and methylophiopogonanone B were purchased from Shanghai Ronghe Medical Technology Development Co., Ltd. (Shanghai, China). 20-Hydroxyganoderic acid G; gano-lactone B; ganoderic acid I; ganoderlactone D; ganoderenic acid C; ganoderic acid C2, (3β,7β,12β,20Z)-3,7,12-trihydroxy-11,15,23-trioxo-lanost-8,20-dien-26-oic acid; ganoderic acid C6; ganoderic acid G; ganoderenic acid B; ganoderic acid N; ganoderic acid B; ganoderic acid LM2; ganoderenic acid A; chol-8-en-24-oic acid,7,15-dihy-droxy-4,4,14-trimethyl-3,11-dioxo-, (5alpha)-; ganoderenic acid E; ganoderic acid A; ganoderic acid H, 20(21)-dehydrolucidenic acid A; deacetyl ganoderic acid F; ganoderic acid D2; 12-hydroxyganoderic acid D; lucidenic acid A; ganoderenic acid D; ganoderic acid D; and ganoderic acid C1 were purchased from Chengdu Pusi Bio-Technology Co., Ltd. (Shanghai, China). LZHCs were obtained from Wuxianji Co., Ltd. (Guangzhou, China). High-performance liquid chromatography (HPLC)- grade formic acid was obtained from Roe Scientific (Newark, United States). HPLC-grade acetonitrile and methanol were obtained from Merck (Darmstadt, Germany). Deionized water was prepared with an ELGA PURELAB flex system (ELGA LabWater, United Kingdom). Analytical-grade n-butanol was from Hangzhou Gaojing Jingxi Chemical Co., Ltd. (Zhejiang, China).

Sample preparation

The contents of LZHC (10 g) were refluxed for 2 h in a water bath with 150 mL water and 40 mL water-saturated n-butanol, and then cooled to room temperature (10°C–30°C) for stratification. The upper layer was collected, subjected to rotary evaporation, and re-dissolved in 70% methanol. The sample was centrifuged at 10,000 rpm for 10 min, and the supernatant was taken for LC-MS analysis.

UPLC-Q-TOF/MS analysis

An Acquity UPLC system (Waters, Milford, United States) coupled with a Triple TOF SYNAPT XS system (Waters, Milford, United States) was employed for chemical identification.

Chromatographic separation was performed on a Waters ACQUITYUPLC HSS T_3 column (100 mm × 2.1 mm,1.8 μm) at a column temperature of 30°C with mobile phase A (water containing 0.05% formic acid; v/v) and mobile phase B (100% acetonitrile). The flow rate was 0.25 mL/min and linear gradient elution was performed under the following optimized conditions: 0 to 8 min, 2% to 2% B; 8 to 15 min,2% to 15% B; 15to 19 min, 15% to 15% B; 19 to 30 min, 15% to 25% B; 30 to

40 min, 25% to 27% B; 40 to 52 min, 27% to 29% B; 52 to 75 min, 29% to 35% B; and 75 to 95 min, 35% to 100% B. The detection wavelength range was set to 190 nm to 400 nm, and the injection volume was 3 μL.

The analysis was carried out in negative-ion mode using the following parameters: scan range, mass/charge *(m/z)* ratio of 50 to 1,200 Da; capillary voltage, 2.5 kV; cone gas flow, 50 L/h; desolvation gas flow, 700 L/h; source temperature, 140°C; desolvation temperature, 20°C; collision energy, low-mass (50 Da) CE ramp (8V–12 V), and high-mass (1,200 Da) CE ramp (60 V-90 V). The MS data was collected in data-dependent analysis mode.

Raw MS data preprocessing

Raw MS data was first preprocessed with Progenesis QI 4.1, Nonlinear Dynamics)[21]. The picking limits were set using a minimum intensity of 15,000 and a minimum width of 0.5 min. Then, the MSP data file and corresponding CSV metadata files (containing compound intensities and annotations) were exported.

Table 1

Parameters used to construct the molecular network.

Workflow selection	Parameter	Value
Basic options	Quantification table source	Progenesis QI
	Precursor ion mass tolerance	0.01
	Fragment ion mass tolerance	0.01
Advanced network options	Min Pairs Cos	0.8
	Network TopK	10
	Minimum matched fragment ions	4
	Maximum connected component size	100
	Maximum shift between precursors	500
Advanced filtering options	Advanced filtering options	Do not filter
	Filter peaks in 50 Da Window	Do not filter
Advanced library search options	Library search min matched peaks	6
	Score threshold	0.7

MN of MS data

MS-MN data for LZHC was generated using the on-line Feature-Based Molecular Networking (FBMN) workflow on the Global Natural Product Social Molecular Networking (GNPS) platform[22–24] (http://gnps.ucsd.edu). Data processing was performed using Progenesis QI software. The parameter settings used to construct the molecular network are shown in Table 1, and the other parameters used were the default parameters recommended on the website. The constructed MN was visualized using Cytoscape software 3.8.0.

Compound target prediction for LZHC

Target information for the tentatively identified compounds was collected from the Swiss Target Prediction database[25] (http://www.swisstargetprediction.ch/). The selection criteria for the compound targets were the top 10 targets with probability >0. The protein-target information obtained was standardized using the UniProt database (https://www.uniprot.org/), and the gene symbols were converted into official HUGO Gene Nomenclature Committee symbols (https://www.genenames.org/).

Duplicate genes were deleted and the target list was uploaded to the Database for Annotation, Visualization, and Integrated Discovery (DAVID; https://david.ncifcrf.gov/). Official gene symbols were selected as identifiers, annotated using *Homo sapiens* as the species, and outputted using "gene list" as the list type. Next, the main LZHC biological processes and metabolic pathways were analyzed by carrying out an enrichment analysis.

LZHC compound-target-pathway networks were generated using Cytoscape software 3.8.0. The built-in software tools were used to analyze different networktopology parameters of the targets, including the degree,

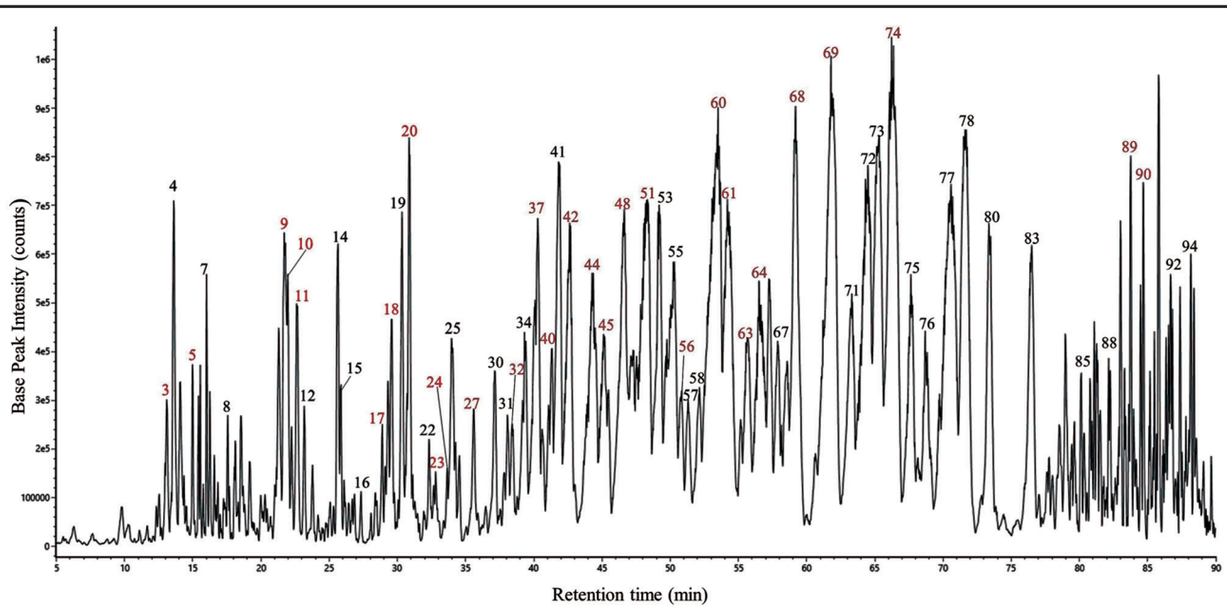

Figure 1. Mass spectrometry chromatogram of an Lingzhihuang capsule obtained in negative-ion mode. Number1–94 represent compounds identified. The red numbers represent compounds identified based on reference compound matching.

betweenness centrality, and closeness centrality, to obtain pivotal targets according to the network parameters.

Results

Characterization of chemical constituents of LZHC by UPLC-Q-TOF/MS and MN

LZHC extract was analyzed by UPLC-Q-TOF/MS, and a representative sample chromatogram generated in negative-ion mode is shown in Figure 1. The raw data was analyzed using Progenesis QI software to obtain an ionfeature quantification table (CSV file) and a corresponding MS/MS spectral summary (MSP file). The LZHC molecular network was constructed using the FBMN pipeline and was searched in the GNPS library. In addition, the compounds were matched with a traditional Chinese medicine library using UNIFI[26] 1.94 (Waters Traditional Medicine Library, Software built-in database), after which the candidate compounds were identified according to the MS data that were automatically extracted by the software, based on matching reference compounds, matches in the literature[27–31], GNPS analysis, and database searches (such as the Reaxys database). Based on the above methods, the 94 LZHC constituents were identified or tentatively characterized, including 58 triterpenoids, 21 flavonoids, eight organic acids, four triterpenoid saponins, one fatty acid, one saponin, and one other compound. The related

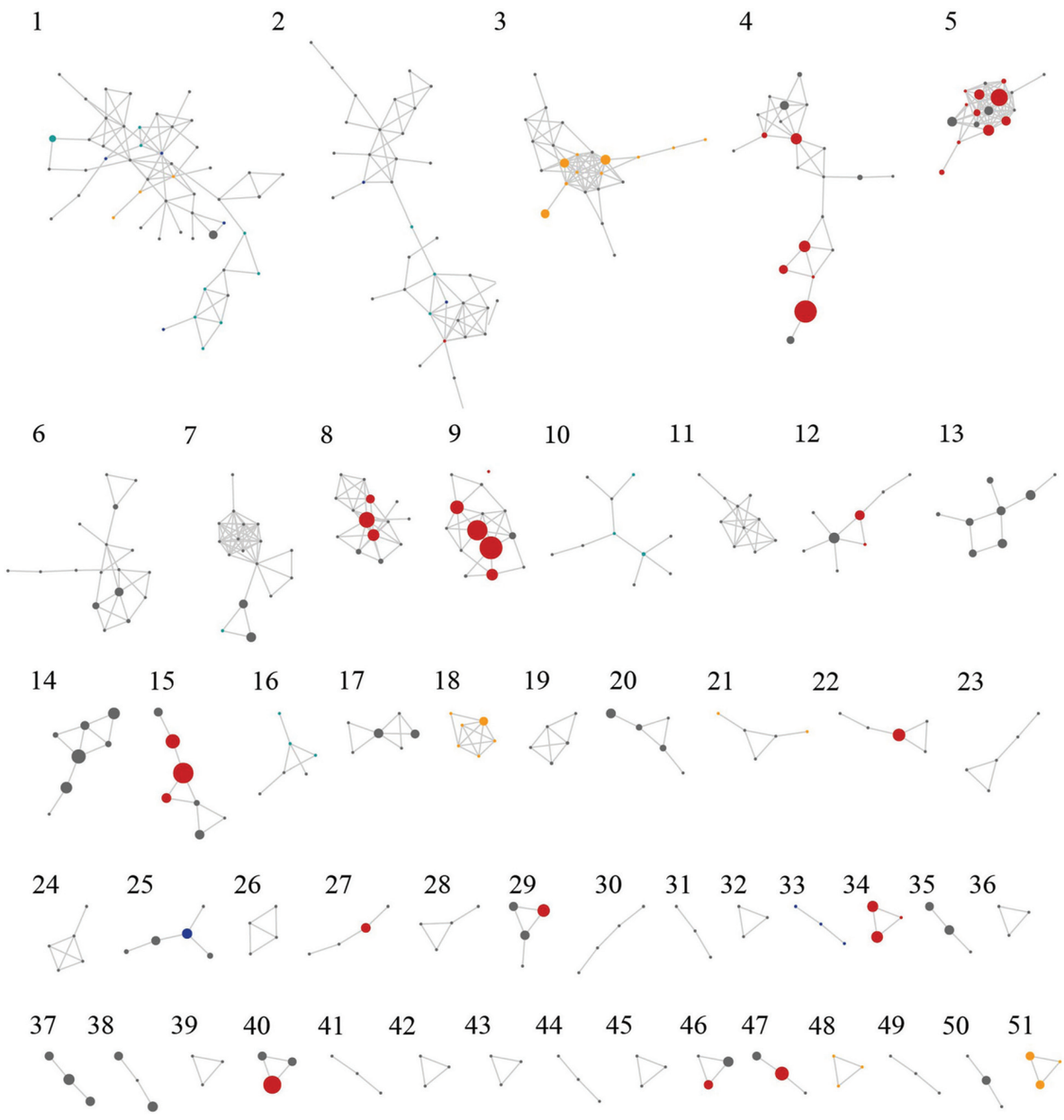

Figure 2. Molecular networking analysis of an Lingzhihuang capsule. In the network, the red nodes represent triterpenoids and the orange nodes represent flavonoids, each node represents the mass spectrometry information of a compound, and hub nodes are represented with a larger node size. The line between nodes represents the correlation between the mass spectrometry spectrum of two compounds. The correlation can be expressed by the thickness of the line.

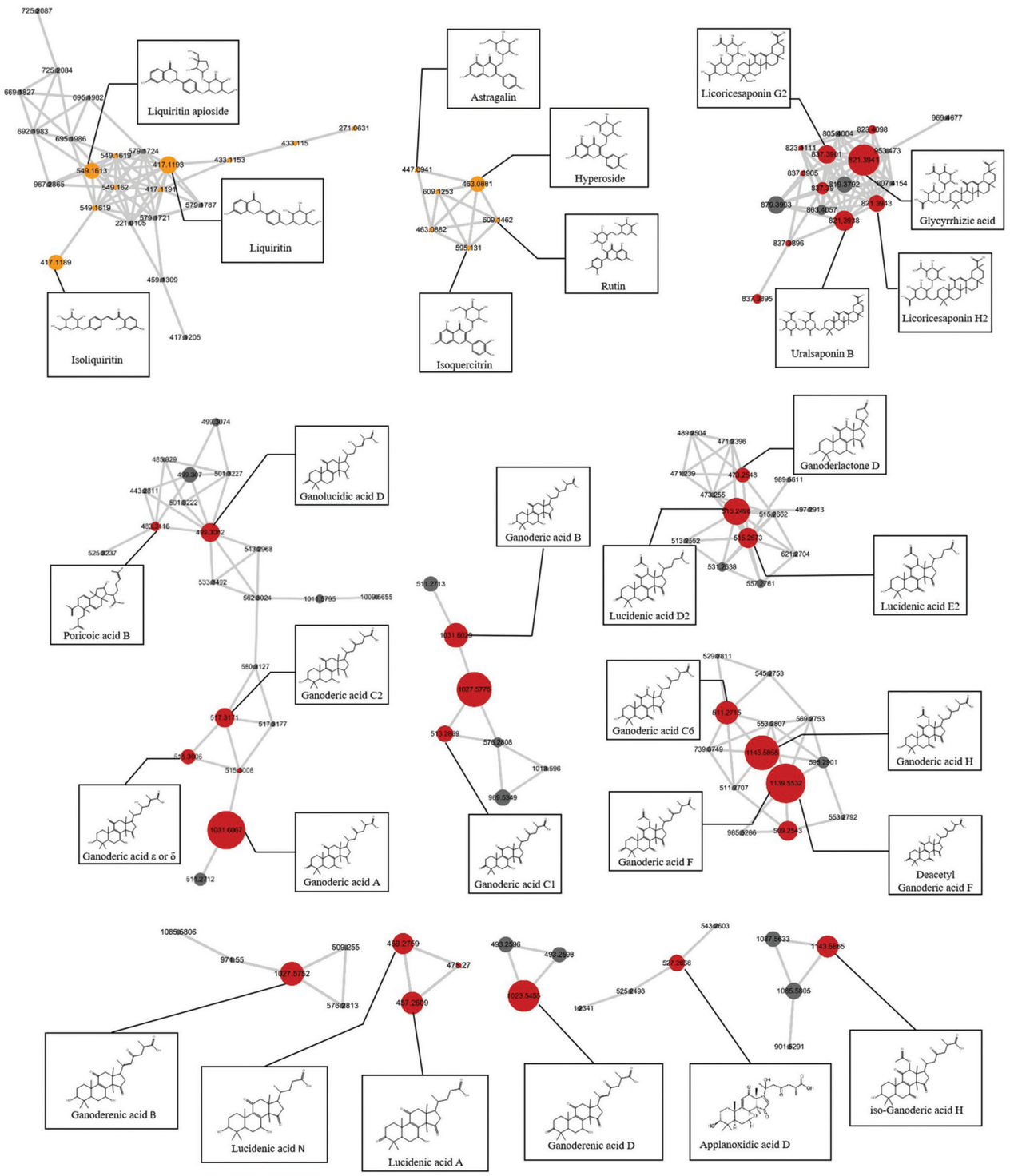

Figure 3. Representative molecular networking clusters of an Lingzhihuang capsule. In the network, the red nodes represent triterpenoids and the orange nodes represent flavonoids, each node represents the mass spectrometry information of a compound, and hub nodes are represented with a larger node size. The line between nodes represents the correlation between the mass spectrometry spectrum of two compounds. The correlation can be expressed by the thickness of the line.

herbs of these chemical constituents were further assigned using the TCMSP platform and information in the literature. The compound-identification results are shown in Table S1, http://links.lww.com/AHM/A6.

The MN was visualized using Cytoscape 3.8.0 and was found to contain 954 nodes and 1,174 edges (Figure 2). The node size corresponds to the ion intensity, and the node color represents the structural category of the compound. The represent compounds were annotated on the nodes, and triterpene was identified as the main structural type, and the other clusters were mainly flavonoids and organic acids (Figure 3).

Target prediction and pathway enrichment for LZHC

The targets of the 94 chemical compounds identified by UPLC-Q-TOF/MS were searched for in the Swiss Target Prediction database, which revealed related targets or all but five of the compounds. The top 10 targets of each compound with probability >0 were retrieved, and the duplicate targets were eliminated, resulting in a list of 165 targets in total. The signaling pathways of LZHC-related targets were analyzed using the DAVID platform, and the results showed that the main biological processes included signal transduction, positive regulation of transcription from the RNA polymerase II promoter, oxidation reduction processes, inflammatory responses, and positive regulation of cell proliferation. The molecular functions of related targets are mainly associated with protein binding, zinc ion binding, ATP binding, protein homodimerization activity, and enzyme binding. The top 10 biological processes, molecular functions, and cellular components were ranked using the number of related genes and then visualized using an on-line bioinformatics tool (http://www.bioinformatics.com.cn) (Figure 4). The main pathways identified included pathways in cancer, proteoglycans in cancer, the PI3K-Akt signaling pathway, and the cAMP signaling pathway (Table 2), indicating the regulatory effects of LZHC on inflammation and cancer.

Compound-target-pathway network for LZHC

An LZHC compound-target-pathway network consisting of 207 nodes and 790 edges was constructed using Cytoscape version 3.8.0 (Figure 5). The topological structure of the network was analyzed, and pivotal LZHC targets were determined according to the topological degree (Table 3). Network analysis shows that the degrees of TNF and NOS2 in the network were 53 and 49, respectively; the betweenness centralities were 0.14 and 0.10, respectively; and the closeness centralities were 0.39 and 0.39, respectively. Thus, our data predicted that TNF and NOS2 are pivotal targets of LZHC. NR3C1, ESR1, SRD5A2, PTGER4, ESR2, PIK3CA, MAPK3, and AKT1 were also identified as relatively important targets. These nodes were found to be regulated by multiple compounds and to act on multiple pathways, which may play an important role in the health-promoting effects of LZHC.

Discussion

In this study, the chemical constituents identified or tentatively characterized in LZHC were mainly triterpenoids and flavonoids, and triterpenoids accounted for the majority. Phenolic acids such as protocatechuic acid, chlorogenic acid, and caffeic acid have significant

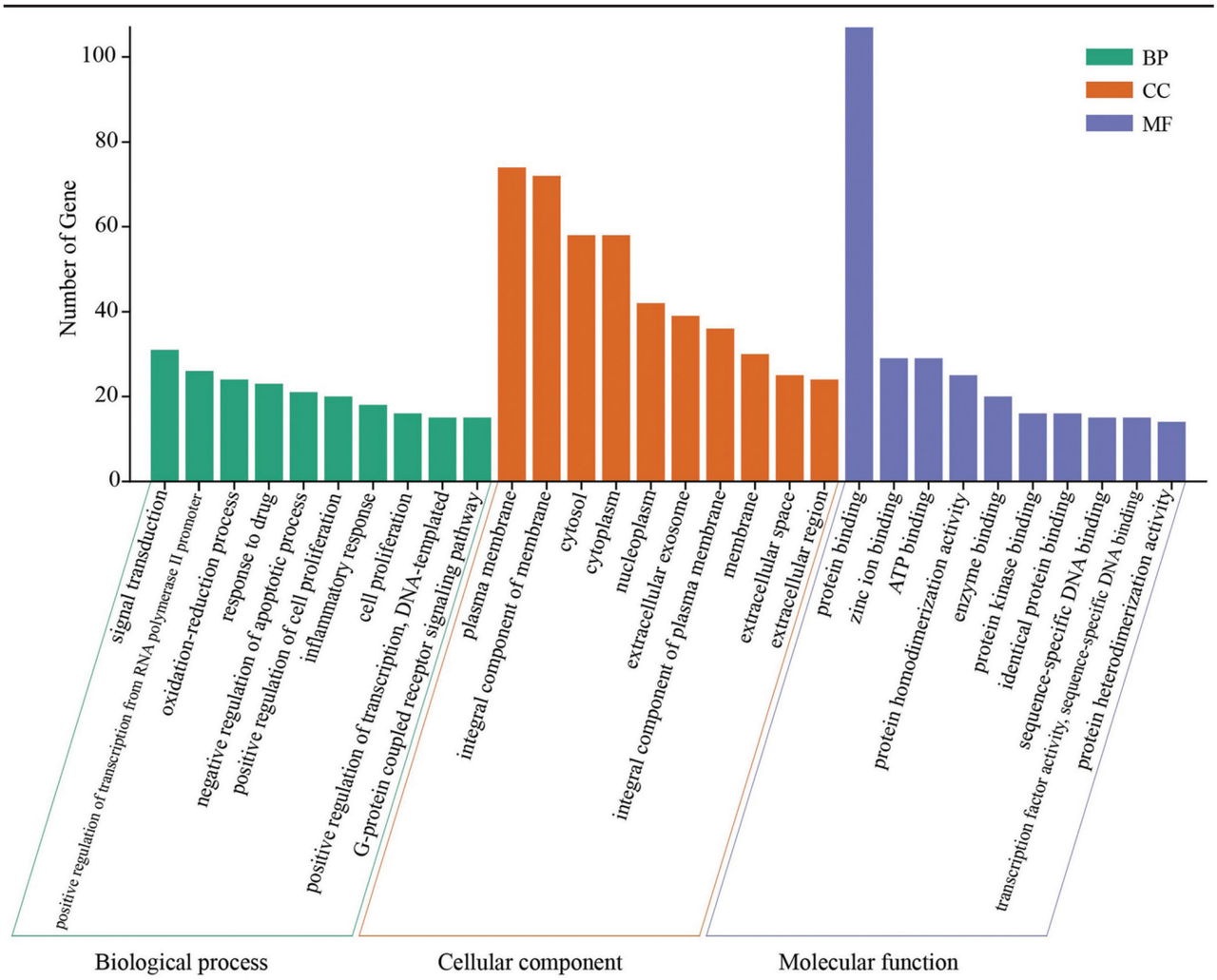

Figure 4. Gene enrichment based on gene ontology analysis.

Table 2

Pathway-enrichment results for Lingzhihuang capsule target pathways.

Pathway number	KEGG pathway	Count	Genes
hsa05200	Pathways in cancer	33	AKT1, AR, BCL2L1, CASP3, CDK2, EGFR, EPAS1, FGFR1, FLT3, GLI1, GSK3B, HSP90AA1, HSP90AB1, IGF1R, JUN, KIT, MAPK3, MDM2, MET, MMP1, MMP2, MMP9, NOS2, PIK3CA, PPARD, PPARG, PTGER1, PTGER2, PTGER3, PTGER4, PTGS2, STAT3, VEGFA
hsa04080	Neuroactive ligand-receptor interaction	22	ADORA1, ADORA3, ADRA2A, ADRA2C, ADRB1, ADRB2, AVPR2, CHRNA7, F2, HTR2B, NMUR2, NR3C1, OPRK1, OXTR, PTAFR, PTGDR, PTGER1, PTGER2, PTGER3, PTGFR, PTGIR, PTGER4
hsa05205	Proteoglycans in cancer	21	AKT1, CASP3, CTSL, EGFR, ESR1, FGFR1, IGF1R, KDR, MAPK3, MDM2, MET, MMP2, MMP9, PIK3CA, PPP1CC, PTPN11, PDPK1, SRC, STAT3, TNF, VEGFA
hsa04151	PI3K-Akt signaling pathway	19	AKT1, BCL2L1, CDK2, EGFR, FGFR1, GSK3B, HSP90AA1, HSP90AB1, IGF1R, IL2, KDR, KIT, MAPK3, MDM2, MET, PDPK1, PIK3CA, PPP2R5A, VEGFA
hsa05215	Prostate cancer	14	AKT1, AR, CDK2, EGFR, FGFR1, GSK3B, HSP90AA1, HSP90AB1, IGF1R, MAPK3, MDM2, PDPK1, PIK3CA, SRD5A2
hsa04931	Insulin resistance	14	AKT1, GSK3B, NR1H3, PDPK1, PIK3CA, PPARA, PPP1CC, PRKCD, PTPN1, PTPN11, PYGL, RPS6KA3, STAT3, TNF
hsa04024	cAMP signaling pathway	14	ADORA1, ADRB1, ADRB2, AKT1, GLI1, JUN, MAPK3, OXTR, PDE4D, PIK3CA, PPARA, PPP1CC, PTGER2, PTGER3
hsa04014	Ras signaling pathway	14	AKT1, BCL2L1, EGFR, FGFR1, IGF1R, KDR, KIT, MAPK3, MET, PIK3CA, PLA2G1B, PLA2G2A, PTPN11, VEGFA
hsa04915	Estrogen signaling pathway	13	AKT1, EGFR, ESR1, ESR2, HSP90AA1, HSP90AB1, JUN, MAPK3, MMP2, MMP9, PIK3CA, PRKCD, SRC
hsa04510	Focal adhesion	13	AKT1, EGFR, GSK3B, IGF1R, JUN, KDR, MAPK3, MET, PDPK1, PIK3CA, PPP1CC, SRC, VEGFA
hsa05206	MicroRNAs in cancer	13	ABCB1, ABCC1, CASP3, CDC25A, CYP1B1, EGFR, MDM2, MET, MMP9, PIM1, PTGS2, STAT3, VEGFA
hsa04914	Progesterone-mediated oocyte maturation	12	AKT1, CCNB3, CDC25A, CDK1, CDK2, HSP90AA1, HSP90AB1, IGF1R, MAPK3, PGR, PIK3CA, RPS6KA3
hsa04015	Rap1 signaling pathway	12	AKT1, EGFR, FGFR1, IGF1R, ITGAL, KDR, KIT, MAPK3, MET, PIK3CA, SRC, VEGFA
hsa00910	Nitrogen metabolism	11	CA12, CA1, CA5B, CA3, CA2, CA5A, CA4, CA7, CA6, CA9, CA14
hsa04726	Serotonergic synapse	11	ALOX15, ALOX5, APP, CASP3, HTR2B, MAOA, MAOB, MAPK3, PTGS1, PTGS2, SLC6A4
hsa04020	Calcium signaling pathway	11	ADRB1, ADRB2, CHRNA7, EGFR, HTR2B, NOS2, OXTR, PTAFR, PTGER1, PTGER3, PTGFR
hsa04722	Neurotrophin signaling pathway	10	AKT1, GSK3B, JUN, MAPK3, PDPK1, PIK3CA, PRKCD, PSEN2, PTPN11, RPS6KA3
hsa05160	Hepatitis C	10	AKT1, EGFR, GSK3B, MAPK3, NR1H3, PDPK1, PIK3CA, PPARA, STAT3, TNF
hsa04068	FoxO signaling pathway	10	AKT1, CCNB3, CDK2, EGFR, IGF1R, MAPK3, MDM2, PDPK1, PIK3CA, STAT3
hsa05161	Hepatitis B	10	AKT1, CASP3, CDK2, JUN, MAPK3, MMP9, PIK3CA, SRC, STAT3, TNF

KEGG: Kyoto encyclopedia of genes and genomes.

anti-inflammatory, anti-oxidant, and anti-viral activities[32–34]. Likewise, flavonoids including liquiritin, liquiritigenin, and licochalcone A have anti-inflammatory, immunomodulatory, anti-tumor, and anti-bacterial effects[35–37]. Furthermore, triterpenes such as 20-hydroxylganoderic acid G, elfvingic acid A, and ganohainanic acid C can significantly enhance macrophage phagocytosis and have immunomodulatory effects[27]. The above compounds complement each other, so it is possible that these compounds are critical for the therapeutic effects of LZHC.

The relationships among chemicals in LZHC and their predicted targets have been rarely reported. Our findings suggested that 49 constituents of LZHC target TNF, 47 target NOS2, and 24 target NR3C1, which indicates that LZHC compounds elicit synergistic effects. TNF is a cytokine that binds to TNFRSF1A/TNFR1 and TNFRSF1B/TNFBR, is mainly secreted by macrophages, and plays important roles in humoral immune responses and systemic inflammation. TNF can also induce cell death in some tumor cell lines[38–39]. NOS2 produces nitric oxide and acts as a biomodulator in various processes, including neurotransmission, anti-bacterial pathways, and anti-tumor pathways. NOS2 can mediate tumor cell death and exert a bactericidal effect on macrophages[40–42]. At present, monoclonal antibodies against TNF-alpha such as infliximab[43], adalimumab[44], etanercept[45], and certolizumab pegol[45] have become powerful drugs for treating rheumatoid arthritis and Crohn's disease. Rao et al.[46] found that infliximab combined with miR-146a synergistically inhibited the proliferation, invasion, and migration of gastric cancer cells. Therefore, it is speculated that the regulation of these targets may be essential mechanisms associated with the therapeutic effects of LZHC.

This study had several limitations. First, the data generated for LZHC may depend on the method used to extract the raw material (extraction with water without using organic solvents). In addition, in the LZHC prescription, *G. lucidum* is the monarch drug, the constituent compounds of which are mainly triterpenes. Importantly, the LZHC contents were extracted with water and n-butanol, and less consideration was given to other constituents, such as volatile compounds in *A. macrocephala* and other medicinal materials. Although the composition of the n-butanol layer was examined, the composition of the aqueous layer was not studied. Thus,

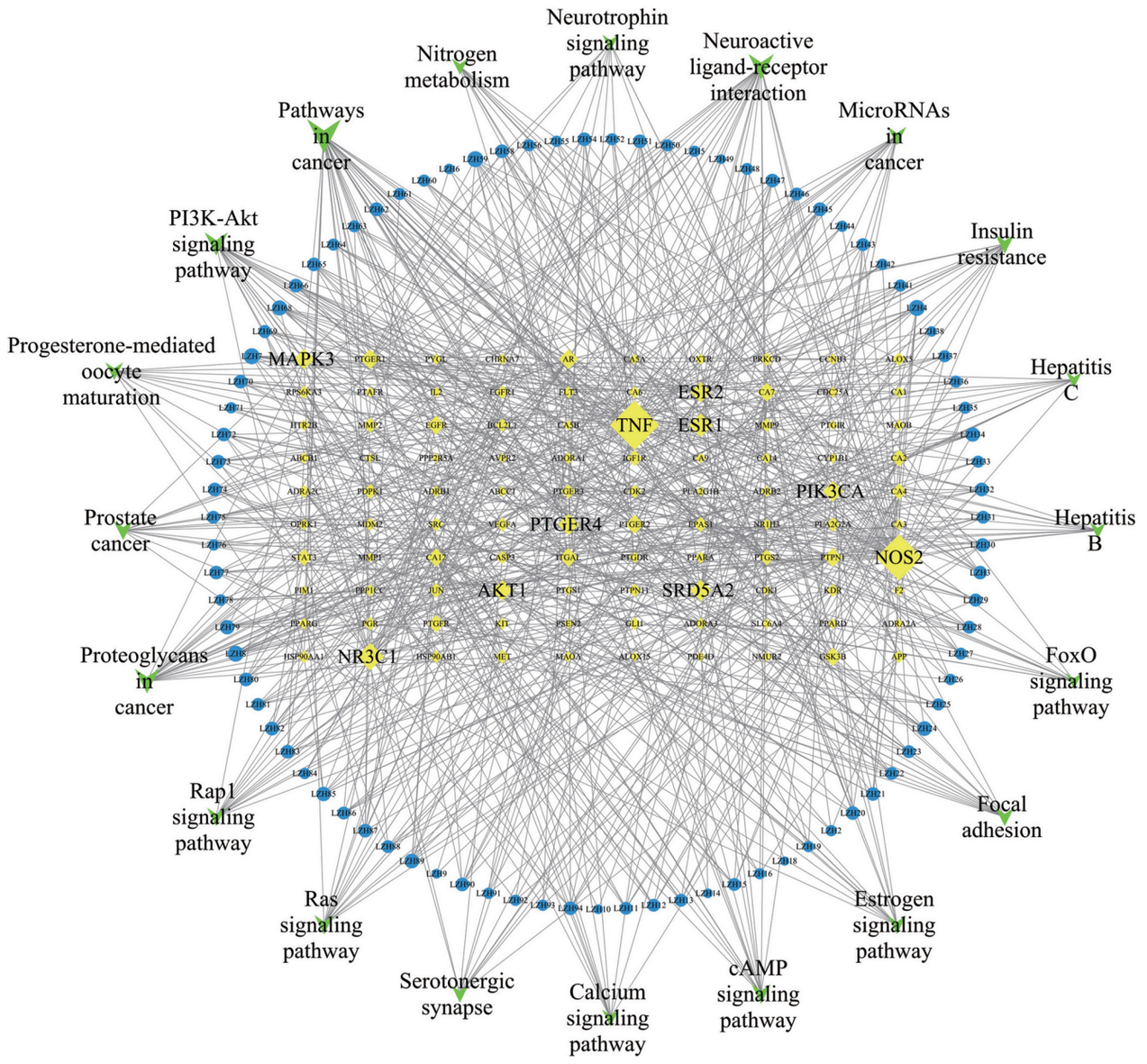

Figure 5. The compound-target-pathway network of an Lingzhihuang capsule. Compounds are indicated with circles, targets are indicated with rectangles, and pathways are indicated with inverted triangles. Hub nodes are represented with a larger node size.

Table 3

Characteristics of the Lingzhihuang capsule target network nodes.

Gene symbol	Degrees	Closeness centrality	Betweenness centrality
TNF	53	0.39	0.14
NOS2	49	0.39	0.10
NR3C1	25	0.34	0.04
ESR1	20	0.35	0.05
SRD5A2	17	0.30	0.01
PTGER4	17	0.35	0.02
ESR2	16	0.33	0.02
PIK3CA	16	0.37	0.02
MAPK3	16	0.38	0.03
AKT1	16	0.37	0.03

AKT1: rac-alpha serine, ESR: estrogen receptor; MAPK3: mitogen-activated protein kinase 3; NOS2: nitric oxide synthase 2; NR3C1: glucocorticoid receptor; PIK3CA: phosphatidylinositol 4,5-bisphosphate 3-kinase catalytic subunit alpha isoform; PTGER4: prostaglandin e2 receptor ep4 subtype; SRD5A2: 3-oxo-5-alpha-steroid 4-dehydrogenase 2; TNF: tumor necrosis factor.

our findings pertaining to the composition of LZHC may not be comprehensive. In addition, the relative proportions of each of the 94 compounds identified in the prescription were not studied, and many compounds in the mass spectrum were detected but not identified, and these compounds should be further studied. Finally, only small molecular components were considered as effective components, but not macromolecular components (such as polysaccharides), which may also play important functional roles and should be investigated in future studies.

Conclusion

In this study, a method for UPLC-Q-TOF/MS analysis was first established to obtain MS data for LZHC. Then, a molecular network was constructed for the MS data based on FBMN, and the chemical constituents of LZHC were identified by various means including MN and matching

with reference compounds. Ninety-four chemical constituents were putatively identified, including triterpenes, flavonoids, and organic acids. The results of compound target prediction and pathway enrichment showed that LZHC may play functional roles in immune regulation, anti-aging, and combination therapy against tumors by regulating potential targets such as TNF, NOS2, NR3C1, ESR1, and AKT1 and related signal pathways, such as pathways in cancer, proteoglycans in cancer, and the PI3K-Akt signaling pathway. These possible mechanisms have been rarely validated in experimental studies, although this topic merits further investigation.

Conflict of interest statement

The authors declare no conflict of interest.

Funding

This project was supported by the Foundation of State Key Laboratory of Component-based Chinese Medicine (Grant No. CBCM2020104).

Author contributions

Mengliang Huang, Qing Shao, and Yi Wang designed the research. Mengliang Huang performed the experimental work. Mengliang Huang, Sijia Yu, and Hao Liu analyzed and visualized the data. Mengliang Huang, Sijia Yu, Hao Liu, Yingchao Wang, and Yi Wang participated in the preparation of the manuscript. Hongzhang Chen and Yansheng Huang provided the research materials. All authors proofread the paper and approved the final version of the manuscript.

Ethical approval of studies and informed consent

Not applicable.

Acknowledgments

None.

References

[1] Das A, Alshareef M, Henderson F, et al. Ganoderic acid A/DM-induced NDRG2 over-expression suppresses high-grade meningioma growth. *Clin Transl Oncol* 2020;22(7):1138–1145.
[2] Wei F, Jiang X, Gao HY, et al. Liquiritin induces apoptosis and autophagy in cisplatin (DDP)-resistant gastric cancer cells *in vitro* and xenograft nude mice *in vivo*. *Int J Oncol* 2017;51(5):1383–1394.
[3] Deng T, Peng D, Yu N, et al. Research progress on chemical composition and pharmacological effects of Poria cocos and predictive analysis on quality markers. *Chin Tradit Herb Drugs* 2020;51:2703–2717.
[4] Zhong LD, Yan PJ, Lam WC, et al. Coriolus versicolor and ganoderma lucidum related natural products as an adjunct therapy for cancers: a systematic review and meta-analysis of randomized controlled trials. *Front Pharmacol* 2019;10:703.
[5] Fei S, Zhang L, He K. The effect and mechanism of Saponins of Radix Glycyrrhiza in mice with acute pancreatitis. *China J Mod Med* 2014;24(19):26–29.
[6] Hong R, Shen MH, Xie XH, et al. Inhibition of breast cancer metastasis *via* PITPNM3 by pachymic acid. *Asian PacJ Cancer Prev* 2012;13(5):1877.
[7] Jiang W, Wang X, Xu X, et al. Effect of Schisandra sphenanthera extract on the concentration of tacrolimus in the blood of liver transplant patients. *Int J Clin Pharmacol Ther* 2010;48(3):224.
[8] Huang Y, Liu X, Tao W, et al. Advances in chemical constituents of *Schisandra chinensis* and activities of anti-type 2 diabetes. *Chin Tradit Herb Drugs* 2019;50:1739–1744.
[9] Wang XT, Yu JH, Li W, et al. Characteristics and antioxidant activity of lignans in *Schisandra chinensis* and *Schisandra sphenanthera* from different locations. *Chem Biodivers* 2018;15(6):e1800030.
[10] Li QS, Chen WH, Zou SY, et al. Clinical observation on the combination of Yanggujian and Lingzhihuang in improving the symptoms of Qi deficiency syndrome. *Hubei J Tradit Chin Med* 2016;3834–3835.
[11] Fu CY, Xia Z, Liu YH, et al. Qualitative analysis of major constituents from Xue Fu Zhu Yu Decoction using ultra high performance liquid chromatography with hybrid ion trap time-of-flight mass spectrometry. *J Sep Sci* 2016;39(17):3457–3468.
[12] Yang B, Wang Y, Tian M, et al. Analysis on chemical constituents of Glycyrrhizae Radix et Rhizoma in Pinelliae Rhizoma Praeparatum by UPLC-Q-TOF-MS/MS. *Chin J Exp Tradit Med Formul* 2017;2345–2349.
[13] Yang B, Dong W, Zhang A, et al. Ultra-performance liquid chromatography coupled with electrospray ionization/quadrupole- time-of-flight mass spectrometry for rapid analysis of constituents of Suanzaoren decoction. *J Sep Sci* 2011;34(22):3208–3215.
[14] Wang ZH, Kim U, Liu JB, et al. Comprehensive TCM molecular networking based on MS/MS in silico spectra with integration of virtual screening and affinity MS screening for discovering functional ligands from natural herbs. *Anal Bioanal Chem* 2019;411(22):5785–5797.
[15] Yang RC, Liu H, Bai C, et al. Chemical composition and pharmacological mechanism of Qingfei Paidu Decoction and Ma Xing Shi Gan Decoction against Coronavirus Disease 2019 (COVID-19): in silico and experimental study. *Pharmacol Res* 2020;157:104820.
[16] Hopkins AL. Network pharmacology: the next paradigm in drug discovery. *Nat Chem Biol* 2008;4(11):682–690.
[17] Li HY, Zhao LH, Zhang B, et al. A network pharmacology approach to deter mine active compounds and action mechanisms of Ge-Gen-Qin-Lian decoction for treatment of type 2 diabetes. *Evid Based Complement Alternat Med* 2014;2014:495840.
[18] Wang Y, Li X, Zhang JH, et al. Mechanism of Xuanfei Baidu Tang in treatment of COVID-19 based on network pharmacology. *China J Chin Mater Med* 2020;45(10):2249–2256.
[19] Li X, Wu LH, Fan XH, et al. Network pharmacology study on major active compounds of Fufang Danshen formula. *China J Chin Mater Med* 2011;36(21):2911–2915.
[20] Wu LH, Gao XM, Wang LL, et al. Prediction of multi-target of Aconiti Lateralis Radix Praeparata and its network pharmacology. *China J Chin Mater Med* 2011;36(21):2907–2910.
[21] Alldritt I, Whitham-Agut B, Sipin M, et al. Metabolomics reveals diet-derived plant polyphenols accumulate in physiological bone. *Sci Rep* 2019;9(1):8047.
[22] Nothias LF, Petras D, Schmid R, et al. Feature-based molecular networking in the GNPS analysis environment. *Nat Methods* 2020;17(9):905–908.
[23] Wang M, Carver JJ, Phelan VV, et al. Sharing and community curation of mass spectrometry data with Global Natural Products Social Molecular Networking. *Nat Biotechnol* 2016;34(8):828–837.
[24] Aron AT, Gentry EC, McPhail KL, et al. Reproducible molecular networking of untargeted mass spectrometry data using GNPS. *Nat Protoc* 2020;15(6):1954–1991.
[25] Daina A, Michielin O, Zoete V. Swiss target prediction: updated data and new features for efficient prediction of protein targets of small molecules. *Nucleic Acids Res* 2019;47(W1):W357–W364.
[26] Wang ZF, Zhao Y, Fan ZQ, et al. Qualitative analysis of chemical constituents in Si-Wu Decoction based on TCM component database. *Acta Pharmaceutica Sinica* 2015;50(10):1309–1317.
[27] Li ZH, Shi YQ, Zhang XH, et al. Screening immunoactive compounds of Ganoderma lucidum spores by mass spectrometry molecular networking combined with *in vivo* zebrafish assays. *Front Pharmacol* 2020;11:287.
[28] Li J, Wang Y, Mei X, et al. Characterization of chemical constituents in aqueous extracts and fermentation broth from Polygonati Rhizoma by UHPLC-LTQ-Orbitrap MS combined with solid phase extraction. *Chin Tradit Herb Drugs* 2019;50:3029–3036. 3043.
[29] Zou YT, Long F, Wu CY, et al. A dereplication strategy for identifying triterpene acid analogues in *Poria cocos* by comparing predicted and acquired UPLC-ESI-QTOF-MS/MS data. *Phytochem Anal* 2019;30(3):292–310.
[30] Zhao Y, Liu S, Zhang C, et al. Analysis on chemical constituents from Glycyrrhizae Radix et Rhizoma by HPLC-Q-TOF-MS. *Chin Tradit Herb Drugs* 2016;47(12):2061–2068.

[31] He X, Yang W, Ye M, et al. Differentiation of *Cuscuta chinensis* and Cuscuta australis by HPLC-DAD-MS analysis and HPLC-UV quantitation. *Planta Med* 2011;77(17):1950–1957.
[32] Song Y, Wang H, Ni F, et al. Study on anti-inflammatory activities of phenolic acids from *Lonicerae japonicae* Flos. *Chin Tradit Herb Drugs* 2015;46(4):490–495.
[33] Ren Q, Ding L, Sun SS, et al. Chemical identification and quality evaluation of Lycopus lucidus Turcz by UHPLC-Q-TOF-MS and HPLC-MS/MS and hierarchical clustering analysis. *Biomed Chromatogr* 2017;31(5):e3867.
[34] Lu YH, Tian CR, Gao CY, et al. Nutritional profiles, phenolics, and DNA damage protective effect of *Lycopus lucidus* Turcz. root at different harvest times. *Int J Food Prop* 2018;20:S3062–S3077.
[35] Rengasamy KRR, Khan H, Gowrishankar S, et al. The role of flavonoids in autoimmune diseases: therapeutic updates. *Pharmacol Ther* 2019;194:107–131.
[36] Kim JK, Oh SM, Kwon HS, et al. Anti-inflammatory effect of roasted licorice extracts on lipopolysaccharide-induced inflammatory responses in murine macrophages. *Biochem Biophys Res Commun* 2006;345(3):1215–1223.
[37] Chueh FS, Hsiao YT, Chang SJ, et al. Glycyrrhizic acid induces apoptosis in WEHI-3 mouse leukemia cells through the caspase- and mitochondria-dependent pathways. *Oncol Rep* 2012;28 (6):2069–2076.
[38] Dubois-Camacho K, Diaz-Jimenez D, De la Fuente M, et al. Inhibition of miR-378a-3p by inflammation enhances IL-33 levels: a novel mechanism of alar min modulation in ulcerative colitis. *Front Immunol* 2019;10:2449.
[39] Wu F, Zhang W, Li L, et al. Inhibitory effects of honokiol on lipopolysaccharide-induced cellular responses and signaling events in human renal mesangial cells. *Eur J Pharmacol* 2011;654 (1):117–121.
[40] Jia J, Arif A, Terenzi F, et al. Target-selective protein S-nitrosylation by sequence motif recognition. *Cell* 2014;159(3):623–634.
[41] Jacenik D, Zielinska M, Mokrowiecka A, et al. G protein-coupled estrogen receptor mediates anti- nflammatory action in Crohn's disease. *Sci Rep* 2019;9(1):6749.
[42] Vuolteenaho K, Koskinen A, Kukkonen M, et al. Leptin enhances synthesis of proinflammatory mediators in human osteoarthritic cartilage-mediator role of NO in leptin-induced PGE(2), IL-6, and IL-8 production. *Mediators Inflamm* 2009;2009 (6):345838.
[43] Gao GH, Li J, Xie HW, et al. Therapeutic effect of infliximab on moderate and severe active rheumatoid arthritis. *J South Med Univ* 2010;30(4):724–726.
[44] Jamal S, Patra K, Keystone EC. Adalimumab response in patients with early versus established rheumatoid arthritis: DE019 randomized controlled trial subanalysis. *Clin Rheumatol* 2009;28(4):413–419.
[45] Arends S, Brouwer E, Efde M, et al. Long-term drug survival and clinical effectiveness of etanercept treatment in patients with ankylosing spondylitis in daily clinical practice. *Clin Exp Rheumatol* 2017;35(1):61–68.
[46] Rao YH, Liang Y, Lu SF, et al. The effects of infliximab combined with miR-146a on gastric cancer cells. *J Mod Oncol* 2019;27:3959–3963.

How to cite this article: Huang ML, Yu SJ, Shao Q, Liu H, Wang YC, Chen HZ, Huang YS, Wang Y. Comprehensive profiling of Lingzhihuang capsule by liquid chromatography coupled with mass spectrometry-based molecular networking and target prediction. Acupunct Herb Med 2022; 2(1):58–67. doi: 10.1097/HM9.0000000000000012